Searching for shared epigenetic clocks: evaluating ultra-conserved markers in a de novo genome assembly of the albacore tuna

Thomas Chevrier, Sylvain Bonhommeau, Michael Thompson, Jessica Farley, Giorgia del Vecchio, Anne-Elise Nieblas, Dominique A Cowart, Julie Imbert Nguyễn, Serge Bernard, Yann Guiguen, et al.

GeroScience
https://doi.org/10.1007/s11357-026-02192-0

ORIGINAL ARTICLE

Searching for shared epigenetic clocks: evaluating ultra-conserved markers in a de novo genome assembly of the albacore tuna

Thomas Chevrier · Sylvain Bonhommeau · Michael Thompson · Jessica Farley · Giorgia Del Vecchio · Anne-Elise Nieblas · Dominique A. Cowart · Julie Imbert Nguyễn · Serge Bernard · Yann Guiguen · Cedric Cabau · Christophe Klopp · Joseph A. Zoller · Steve Horvath · Robert Brooke · Ake T. Lu · Matteo Pellegrini · Jérémie Chanut

Received: 1 February 2026 / Accepted: 3 March 2026

Abstract Accurate age estimation is key to understanding life history, population ecology, and effective management of valuable commercial and ecologically relevant species. While DNA methylation-based epigenetic clocks are well developed in mammals, their application in fish is limited. In contrast to mammals, fish lack identified universal fish epigenetic markers. Here we explore the potential of ultra-conserved elements (UCEs) as age predictor markers in albacore tuna (*Thunnus alalunga*), a worldwide distributed and commercially valuable teleost fish. We produced a de novo reference genome of the albacore tuna in order to facilitate accurate mapping of bisulfite sequencing reads and identify conserved genomic regions. From muscle tissue samples spanning an age range of 0.03 to 17.69 years, we profiled methylation at UCEs and

T. Chevrier (✉) · A.-E. Nieblas · D. A. Cowart · J. Chanut
Company for Open Ocean Observations and Logging (COOOL), Saint-Leu, La Réunion, France
e-mail: t.chevrier.cooolresearch@gmail.com

A.-E. Nieblas
e-mail: anne.elise.nieblas@company-coool.io

D. A. Cowart
e-mail: d.cowart.cooolresearch@gmail.com

T. Chevrier · S. Bonhommeau · J. I. Nguyễn
UMR Entropie - IFREMER - IRD - Université de La Réunion, F-97420 Le Port, La Réunion, France
e-mail: sylvain.bonhommeau@ifremer.fr

J. I. Nguyễn
e-mail: Julie.imbert@ifremer.fr

M. Thompson · G. Del Vecchio · M. Pellegrini
Department of Molecular, Cell and Developmental Biology, University of California, Los Angeles, CA, USA
e-mail: mjthompson69@gmail.com

G. Del Vecchio
e-mail: giodelv@g.ucla.edu

M. Pellegrini
e-mail: matteope@gmail.com

J. Farley
CSIRO Environment, Hobart, TAS, Australia
e-mail: Jessica.Farley@csiro.au

S. Bernard
LIRMM-CNRS, University of Montpellier, Rue Ada, 34000 Montpellier, France
e-mail: serge.bernard@cnrs.fr

Y. Guiguen
INRAE, LPGP, 35000 Rennes, France
e-mail: yann.guiguen@inrae.fr

C. Cabau
Sigenae, GenPhySE, Université de Toulouse, INRAE, ENVT, 31326 Castanet-Tolosan, France
e-mail: Cedric.Cabau@inrae.fr

C. Klopp
Université Fédérale de Toulouse, INRAE, Sigenae, 31326 Castanet-Tolosan, BioinfOmics, France
e-mail: christophe.klopp@inrae.fr

J. A. Zoller
Department of Biostatistics, Fielding School of Public Health, University of California, Los Angeles, CA, USA

Published online: 24 March 2026

identified loci whose methylation levels were strongly correlated with age. By selecting an optimized subset of these regions, we constructed an epigenetic clock that predicts age with a median absolute error of 0.88 years. This demonstrates that UCEs represent a conserved set of age markers in teleosts and supports their potential for constructing shared epigenetic clocks between teleost species. To complement the clock construction, we conducted the first epigenome-wide association study (EWAS) of age in a fish species, enabling a broader characterization of age-associated methylation patterns beyond the CpGs included in the predictive model. This epigenetic aging strategy offers a non-lethal, field-applicable solution to age estimation from small tissue biopsies, avoiding otolith sampling and reducing the resources required to develop species-specific clocks.

Graphical Abstract

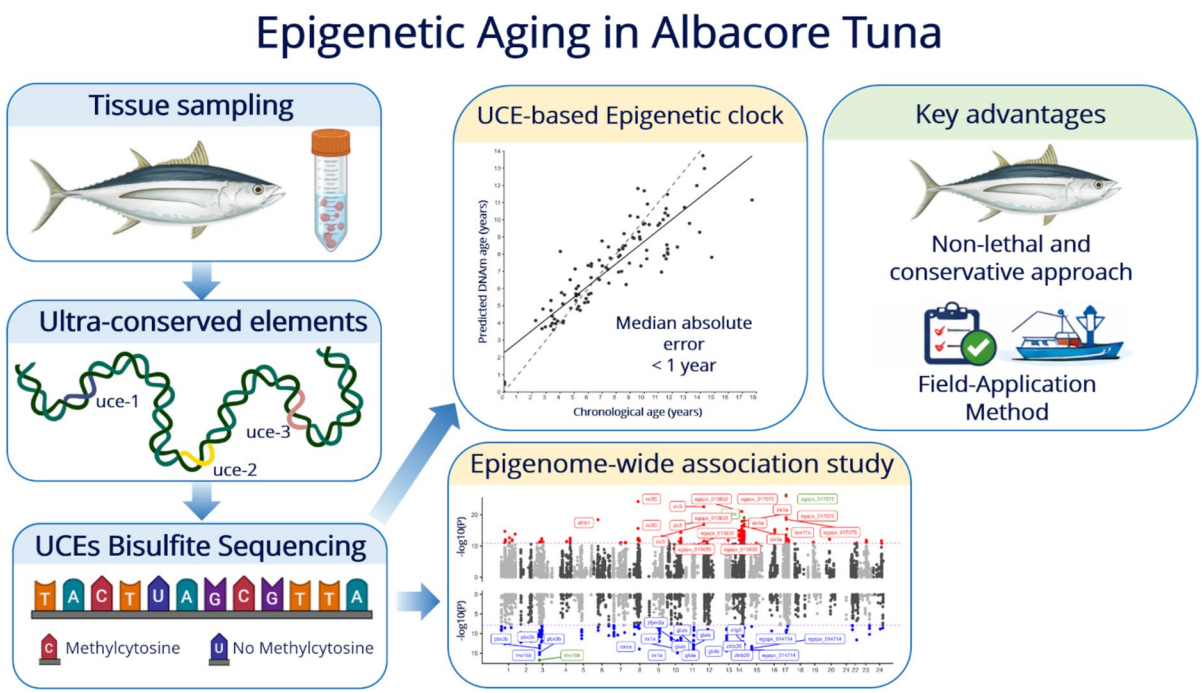

S. Horvath
Department of Human Genetics, David Geffen School of Medicine, University of California, Los Angeles, CA, USA
e-mail: profstevehorvath@gmail.com

S. Horvath · A. T. Lu
Altos Labs, San Diego, USA

S. Horvath · R. Brooke
Epigenetic Clock Development Foundation, Torrance, CA, USA
e-mail: brooke@clockfoundation.org

Keywords Epigenetic · Ultra-conserved elements · Clock · Aging · Epigenome-wide association study

Introduction

Accurately determining the age of individuals is a cornerstone of ecological and biological research. Age information underpins a wide range of applications, from assessing population dynamics to evaluating ecosystem health [1]. Reliable age estimates are essential

for inferring key life-history traits such as growth rates, age at sexual maturity, and age-specific fecundity [2–4]. Consequently, the ability to estimate age enables more robust monitoring of demographic parameters, including population age structure and reproductive potential. Despite its central role, chronological age remains difficult to determine in wild animal populations, particularly in species lacking clear aging markers in hard structures (e.g., vertebrae, otoliths, and teeth) or with limited access to long-term observational data [5, 6].

The importance of chronological age for wild populations has prompted the development of many estimation methods [6]. Morphological features of internal structures have been commonly used to provide accurate age estimation (e.g. mammalian teeth [7]). For fish, age is traditionally determined by counting growth zones in a range of hard structures including otoliths, vertebrae, scales, and fin rays [6, 8, 9]. Such techniques have, however, some shortcomings: they can be costly and time consuming [10], of low accuracy for some species, require inter-calibration and cross-validation between labs, and are necessarily lethal in the case of otolith and vertebra readings [6, 11]. The demand for fish age composition data is increasing, in age-structured stock assessment models, which are essential for estimating key demographic parameters such as recruitment, mortality, growth, and for informing sustainable management of wild fish populations [10, 12–14]. This highlights the need to develop non-lethal methods for accurately estimating chronological age, not only for rare or endangered species where lethal sampling is not feasible, but also to address broader requirements of cost-effectiveness, speed, scalability, and standardization that are critical for fisheries and resource management.

Biological aging is a widespread process across animal species and is typically accompanied by molecular modification [15, 16]. However, evidence of aging impact and senescence in fish remains limited. Unlike most vertebrates, several fish species show no-age related telomere shortening, raising questions about how aging manifests in this taxa [17, 18]. Among the molecular processes associated with aging, DNA methylation at cytosine-phosphate-guanine (CpG) sites has been shown to change with age [19–23]. Methylation profiles have been used to develop biomarkers of age known as epigenetic clocks, which predict chronological age with remarkable accuracy [21, 24–27]. These clocks typically rely on consistent patterns of age-associated hyper- or hypomethylation at specific CpG sites across the genome. This genetic method is promising for inferring biological age. Epigenetic clocks were first built to monitor human aging [21, 25], but their underlying principles appear to be evolutionarily conserved, as they have now been successfully developed for many mammalian species [28, 29]. More recently, a mammalian methylation array was developed by [24], which is a single custom array that measures up to 36 k CpGs per species that are well conserved across many mammalian species [26].

Only a handful of epigenetic clocks have been developed for laboratory-raised fishes, including for European sea bass (*Dicentrarchus labrax*; [11]) and zebrafish (*Danio rerio*; [30]). Further, [31] presented a novel epigenetic age method estimation for two wild-caught reef fish from the Gulf of Mexico (Red snapper: *Lutjanus campechanus* and red grouper: *Epinephelus morio*) while more recently advancing the development of epigenetic clocks in two marine species, a deepwater teleost and a ray [32, 33]. Weber et al., 2024a demonstrated through 61 individuals of the blackbelly rosefish (*Helicolenus dactylopterus*), two single-tissue epigenetic clocks developed from fin clip and muscle tissues showed high correlation ($R^2 > 0.98$; MAE < 1 year) between epigenetic and chronological age. However, a multi-tissue clock with both tissues showed lower performance, particularly for muscle samples ($R^2 = 0.77$; MAE = 5.43 years), indicating tissue-specific differences in age-associated DNA methylation patterns for the targeted region in this species. By contrast, two single tissue (fin clip and whole blood) and a multi-tissue epigenetic clocks were developed for 42 cownose ray (*Rhinoptera bonasus*) achieving high accuracy ($R^2 = 0.97–0.99$; MAE < 1 year; Weber et al. [33]).

In this study, we focus on albacore tuna (*Thunnus alalunga*), which is a commercially important species in all oceans. For this species, age is estimated using otolith readings with high confidence and to decimal-year precision [34, 35], providing a robust basis for calibrating epigenetic age models. Within the framework of stock assessments, the development of an epigenetic clock presents an opportunity to refine estimates of this and other life history parameters. Developing this clock would facilitate the upscaling of sample sizes by enabling the use of small muscle biopsies, which are easier and less expensive to collect than otoliths, and do

not require specialized dissection skills, an important advantage when working with high-value species such as tuna that are commonly sold as whole fish (with the head).

Because developing species-specific epigenetic clocks are resource-intensive, identifying conserved epigenetic markers across species could enable shared clocks and facilitate calibration for new species [24, 26, 36]. In fish, ultra-conserved elements (UCEs) are sequences that remain nearly identical across multiple teleost species despite millions of years of divergence [37, 38]. To this end, a targeted bisulfite sequencing approach was developed to focus on UCEs found in fish [37, 38] to investigate potential common epigenetic clocks for a large number of fish species, starting with albacore tuna. For this purpose, we also generated a de novo reference genome assembly for albacore tuna, as this resource was not yet available for the species, while several high-quality reference genomes have already been published for other tunas, including bigeye tuna (*Thunnus obesus*) (PRJEB71914), Pacific bluefin tuna (*Thunnus orientalis*) [39], southern bluefin tuna (*Thunnus maccoyii*) (PRJEB46021), Atlantic bluefin tuna (*Thunnus thynnus*) (PRJEB72088), and yellowfin tuna (*Thunnus albacares*) (PRJEB47267). Establishing this genomic approach was therefore a necessary step to enable accurate mapping of bisulfite sequencing reads and to ensure reliable identification of conserved epigenetic markers for this species. Epigenetic clocks, built using penalized regression frameworks, focus exclusively on a subset of CpG sites that allow prediction of chronological age. As a result, many CpGs that exhibit age-related variation are not retained in the final models. To obtain a more comprehensive view of age-associated methylation dynamics, we also performed an epigenome-wide association study (EWAS) of age, which is applied in amphibians and mammals [26, 40, 41] but not previously undertaken in fish. Beyond identifying individual CpGs associated with ageing, our objective was also to characterize the biological pathways and functional gene sets linked to these loci in order to evaluate whether fish exhibit molecular ageing signatures analogous to those described in mammals, such as enrichment at Polycomb Repressive Complex 2 (PRC2) target sites or regions marked by H3K27me3 [26, 40, 41].

Materials and methods

Sample collection and chronological age estimation

Muscle samples ($n = 101$) were collected from wild-caught albacore tuna between 2013 and 2014 as part of the GERMON project [42] at three sites in the western Indian Ocean (Reunion, Seychelles, South Africa). Otoliths were collected from these individuals and subsequently read to provide the chronological age information [35]. To improve the accuracy and biological consistency of these age estimates, we applied the *Jesstimation* approach [34], which refines decimal ages by integrating both the number of opaque zones and a daily growth relationship between otolith size and age. Moreover, complete otoliths were weighted to the nearest 0.001 g. Four additional larvae were collected during an Ifremer scientific survey north of La Réunion in January 2022 and age was estimated to be 10 days based on their length (Fig. 1).

DNA extraction

Sample for whole genome and RNA-seq for reference genome

Due to the absence of a complete reference genome for albacore tuna, we undertook de novo genome

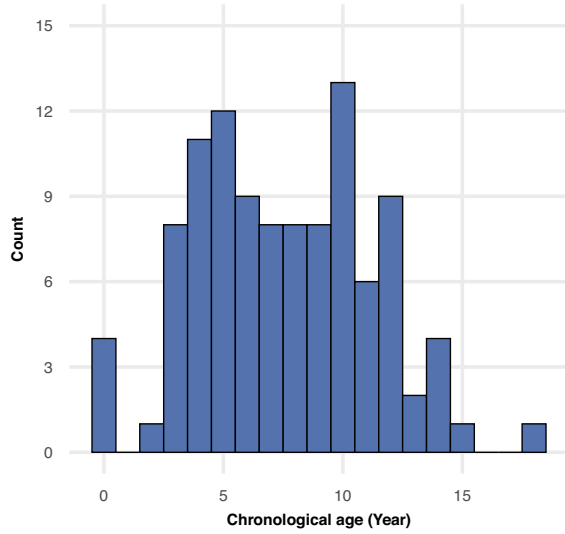

Fig. 1 Total number of samples and age ranges used for albacore tuna UCE clock

sequencing as part of this study. To ensure comprehensive genomic representation, multiple tissue types were sampled, including liver, blood, and kidneys of a male albacore caught in the wild on February 2021 off Reunion Island. Tissue samples were immediately flash-frozen in liquid nitrogen and stored at –96 °C. Genomic DNA was extracted from blood and RNA from kidneys and liver for genome annotation.

Samples for epigenetic profiling

Genomic DNA was extracted from muscle tissue for 101 individuals and from the eyes for four larvae (see Supplementary Fig. 1), using the DNeasy Blood & Tissue Kit (Qiagen), following the manufacturer's protocol. DNA concentrations were quantified with a Qubit™ 4 Fluorometer (Invitrogen™), and DNA purity was assessed using the 260/280 absorbance ratio measured with a NanoDrop Lite spectrophotometer (Thermo Scientific). Samples yielding more than 500 ng and exhibiting a 260/280 ratio between 1.8 and 2.0 were considered as high-quality and retained for subsequent sequencing.

Larvae species identification

Molecular analysis of early developmental stages was essential, as tuna larvae exhibit highly similar morphological features that render visual identification unreliable. To overcome these limitations, a genetic approach was employed to enable accurate species identification. Employing PCR amplification, species-specific primers developed by [43] were applied using the following primer pair: forward primer -GTTTCGTGATCCTGC TAGTG- and reverse primer -CCTCCTAGTTTGTTG GAATAGAT-. PCR was performed under the following thermal cycling conditions: an initial denaturation at 94 °C for 2 min, followed by 35 cycles of denaturation at 94 °C for 30 s, annealing at 55 °C for 30 s, and extension at 72 °C for 30 s, with a final extension step at 72 °C for 3 min, and a final hold at 4 °C. PCR amplification was followed by 2% agarose gel electrophoresis.

Library preparation and sequencing

Whole genome and RNA-seq for reference genome

Genomic DNA quality and concentration were assessed by capillary electrophoresis using the FemtoPulse system (Agilent) and quantified with Qubit (Thermo Fisher Scientific). PacBio HiFi libraries were subsequently prepared following the standard Sequel II protocol, and sequencing was performed on a Sequel II SMRT Cell.

RNA-seq libraries were prepared from total RNA using Universal Plus mRNA-seq kit (NuGEN), which includes poly(A) RNA selection, cDNA synthesis, adaptor ligation and PCR amplification. Library quality was assessed by fragment size distribution on a Fragment Analyzer (High Sensitivity NGS kit, Agilent) and qPCR using a LightCycler 480 (Roche). Sequencing was performed on an Illumina NovaSeq 6000 platform using Sequencing by Synthesis (SBS) chemistry with the NovaSeq Reagent Kit and an SP flow cell. Sequencing data was processed with the NovaSeq Control Software for image analysis, followed by base calling with Real-Time Analysis 3 (RTA3) and demultiplexing using *bcl2fastq* to generate FASTQ files. Read quality was evaluated using the Sequencing Analysis Viewer and FastQC, while potential contaminants were screened with FastQ Screen.

HiFi and Hi-C reads were assembled using Hifiasm version 0.16.1 [44] with default parameters and the resulting contigs were purged using *purge_dups* version 1964aaa [45]. The purged contigs were scaffolded using Hi-C as a source of linking information. Hi-C reads were aligned to the draft genome using Juicer version 1.6 [46] with the -S early parameter. A candidate assembly was generated using the 3D de novo assembly pipeline 3D-DNA version 180,114 [47] with the –early-exit parameter. Finally, the candidate assembly was manually reviewed using the Juicebox assembly tools version 2.13.05 [48]. The genome assembly was screened for adaptor and vector contamination using the NCBI FCS-adaptor pipeline version 0.5.5 (https://github.com/ncbi/fcs). Additional screening against foreign organism contamination was performed with FCS-GX version 0.5.5 [49]. The cleaned assembly was annotated using EGAPx version 0.4.0-alpha, integrating both custom short-read and long-read transcriptomic data and the publicly available library SRR4436658 (https://github.com/ncbi/egapx). The tools mentioned above were all run using their default parameters. Annotation quality and completeness were evaluated with BUSCO version 5.7.1 (Actinopterygii lineage, protein mode) [50], OMArk version 0.3.0 (LUCA.h5 OMA

database, Teleostei clade) [51] and PSAURON version 1.0.2 [52].

Epigenetic profiling

An initial set of candidate probe sequences targeting UCEs in fish genomes was obtained from the UCE website (https://www.ultraconserved.org) [38]. Specifically, probe datasets corresponding to Actinopterygians and Acanthomorphs were downloaded, merged into a single pool, and submitted to Integrated DNA Technologies (IDT) for evaluation.

IDT screened the probe sequences using a dc-megablast alignment approach, applying a 90% sequence identity threshold over at least 50% of the probe length. Probes with zero or more than two genomic hits were excluded based on alignment quality metrics, including e-value and bit score thresholds. To assess probe conservation and specificity across species, the bit scores for each probe were averaged across three representative fish genomes. A perfect alignment across species was defined by a bit score of 217, indicating 100% sequence identity without mismatches or gaps. Based on these metrics, we selected the top 2,999 probes, including both highly conserved and moderately variable sequences (e.g., average scores around 192, reflecting 4—7 mismatches and 1—3 gaps), to create our final custom targeted bisulfite sequencing (TBs-seq) panel.

For library preparation, 500 ng of genomic DNA was fragmented and subjected to end-repair, dA-tailing, and adapter ligation using the NEBNext Ultra II DNA Library Prep Kit (New England Biolabs) with custom pre-methylated adapters (custom adapter plate, IDT). Pools of 16 purified libraries were hybridized to the biotinylated probe panel following the manufacturer's instructions (xGen Hybridization Capture Kit, IDT).

Captured DNA was treated with sodium bisulfite using the EZ DNA Methylation-Gold Kit (Zymo Research), followed by PCR amplification with KAPA HiFi Uracil + ReadyMix (Roche) under the following conditions: initial denaturation at 98 °C for 2 min; 14 cycles of 98 °C for 20 s, 60 °C for 30 s, and 72 °C for 30 s; final extension at 72 °C for 5 min; hold at 4 °C.

Library quality was assessed using the High Sensitivity D1000 Assay on a 4200 Agilent TapeStation. Libraries were pooled (96 per pool) and sequenced as 150 bp paired-end reads on an Illumina NovaSeq 6000 (S1 flow cell).

Methylation data analysis

As a consequence of the bisulfite treatment, standard alignment approaches are unsuitable for bisulfite-converted sequencing data. To address this, a bisulfite-specific reference index was constructed using BiSulfite Bolt (*BS Bolt*) [53] by converting the albacore reference genome to represent all possible bisulfite-induced C-to-T and G-to-A transitions on both DNA strands. FastP [54] was used to trim adapter sequences, exclude short reads (<=40 bp), trim read ends if base-calling quality moving average fell below phred=15, and "deduplicate" the data by removing 100% identical copies of unique sequences. Filtered FASTQ files were then aligned to the bisulfite-indexed reference genome using BS Bolt. which utilizes a modified version of *BWA MEM* [55, 56] tailored for alignment of bisulfite sequencing data. Reads were in silico bisulfite converted, modifying unconverted methylated bases, and subsequently mapped to the bisulfite alignment index of the reference genome. Finally, read alignments were assessed for mapping quality and bisulfite uniqueness. Resulting alignment files were in BAM format. As recommended by [53], a pre-processing step was carried out using *samtools* [57] to remove duplicates. Using *BS Bolt*, methylation calling generated a CGmap file that included all mapped reads at each CG not marked as PCR duplicates. A methylation matrix was generated from the CGmap files obtained for all samples.

Statistical modelling for age prediction from methylation profiles

Hierarchical clustering of the full albacore tuna dataset (Supplemental Fig. 2) using *pheatmap* (v.1.0.13) showed no grouping by sex and revealed no individuals with markedly divergent methylation profiles. This indicates a relatively uniform epigenetic landscape across samples, with no strong sex effects or outliers driving global variation. To evaluate the potential of UCE-associated DNA methylation profiles for age prediction in tuna, we constructed age estimators using elastic net regression (alpha=0.5), with chronological age as the response variable, natural log transformed to account for non-linear trends

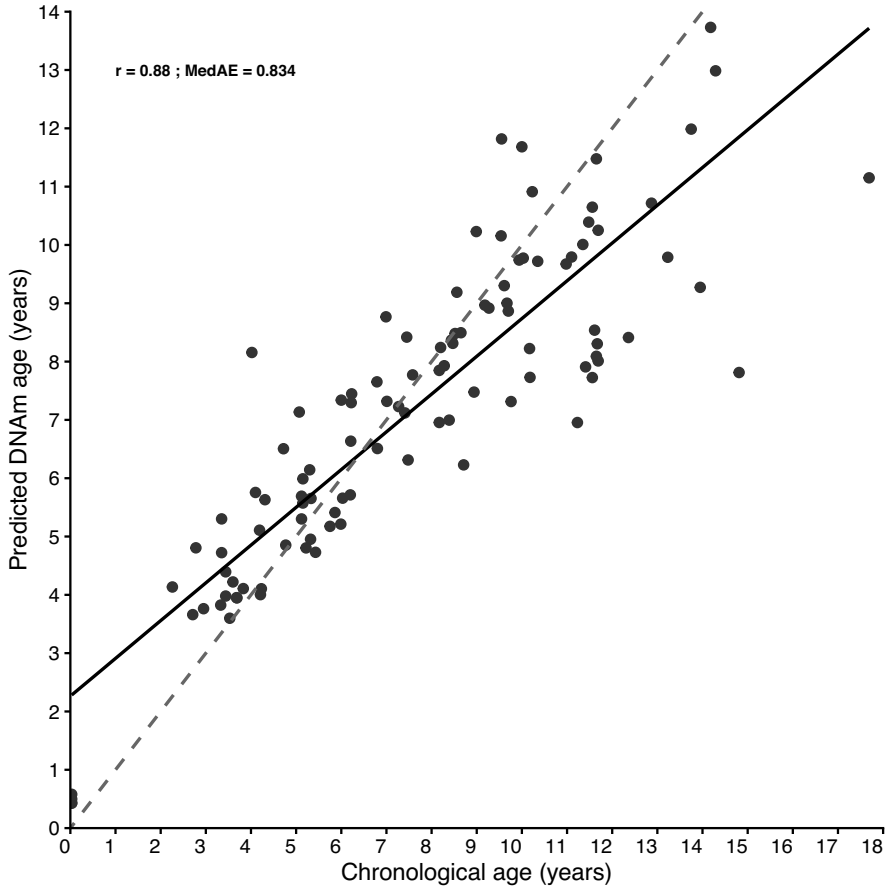

Fig. 2 Leave-one-out cross validation study of the UCE epigenetic clock for albacore tuna, *Thunnus alalunga*

between methylation and age, and CpG methylation levels as predictors. Models were implemented using the *MammalMethylClock* (v1.0.0) R package [58]. To assess model performance, we conducted leave-one-out cross-validation (LOOCV). In each iteration, one sample was excluded from the training set, and a model was built on the remaining samples to predict the age of the held-out sample. This process was repeated across all samples to generate a full set of predicted ages. Model accuracy was evaluated by calculating the Pearson correlation coefficient (R) between predicted and otolith-derived ages, as well as the median absolute error (MedAE; in years).

Epigenome-wide association study with age

We conducted an EWAS of age on the 7,637 CpGs mapped to the de novo albacore genome. Association analyses were performed in *R* using the *standardScreeningNumericTrait* function from the WGCNA package (v1.73) [59]. The relationship between chronological age and CpG methylation levels was assessed using the Pearson correlation.

Genomic coordinates for all CpG sites were derived from their identifiers and converted to BED format. CpGs were mapped to genomic intervals using the *GenomicRanges* package (v1.60.0). Each CpG was represented as a 1 bp interval centered on its genomic position, with an additional 1 bp padding on each side. Gene models were obtained from our *Thunnus alalunga* de novo reference annotation (GFF3 format), which was imported using *rtracklayer* (v1.68.0) and processed with *GenomicFeatures* (v1.60.0) to construct a transcript database (TxDb). Gene identifiers from the TxDb object were mapped to corresponding GFF3 gene entries through nearest-neighbour and overlap-based matching. For each annotated gene, strand-specifically transcription start sites (TSSs) were defined and used to generate regulatory domains following the basal-plus-extension

model implemented in *rGREAT* (v2.10.0), a tool designed for functional and biological pathway annotation of genomic regions. Specifically, regulatory regions comprising 5 kb upstream and 1 kb downstream of each TSS, extended up to 250 kb when no other gene boundary was encountered. The maximum extension distance was set to 250 kb, rather than the default 1 Mb used in *rGREAT*, as the latter is defined based on the human genome. Given that the human genome is approximately four times larger than our de novo assembled tuna genome, we applied a proportional scaling to define an extension distance of 250 kb. Ultraconserved elements (UCE)-overlapping CpGs were assigned to genes whose regulatory domains overlapped the CpG intervals. CpGs overlapping multiple regulatory domains were counted for each associated gene in the enrichment analysis. Gene-level metadata (gene symbol, locus tag, and functional annotations) were extracted directly from the GFF3 file to build a comprehensive annotation table associated with each mapped CpG. All genomic intervals and regulatory domain assignments were saved as GRanges objects for downstream enrichment analyses.

GREAT-like enrichment analysis was achieved using *msigdbr* (v25.1.1) to the top 150 positively and the top 150 negatively age-related CpG sites from the EWAS of age. Our framework implements foreground/background hypergeometric tests, using all annotated CpGs as the background and the genomic regions of the top 150 positively and the top 150 negatively age-related CpG as the foreground. The GREAT-like analysis was carried out on the same biological pathways and functional gene sets used in [26] (Disease ontology, GO Biological process, Human phenotype, MSigDB pathway, MSigDB perturbation and GO molecular function) to highlight any possible analogy with the enrichment observed in mammals.

Results

Whole genome sequencing

The genome assembly of the albacore tuna represents the first chromosomal-scale reference available for this species. The initial assembly, generated using Hifiasm from PacBio HiFi long reads, resulted in 537 scaffolds, with a scaffold N50 of 3.6 Mb, reflecting a high level of sequence continuity. In a second step, we used Hi-C contact maps to scaffold and organize the assembly, resulting in a complete scaffolded genome comprising 38 scaffolds, with a markedly improved scaffold N50 of 34.1 Mb. Of these, 24 scaffolds correspond to chromosome-scale scaffolds, consistent with the expected haploid chromosome number ($n = 24$) previously reported in tunas [60], into which Hi-C integration enabled anchoring of 99.88% of the 785.3 Mb genome sequence. Genome annotation identified 24,013 protein-coding genes and 33,813 transcripts, supported by 427,392 exons and 404,261 coding sequences (CDS). Assembly completeness and annotation quality were confirmed by multiple assessments: BUSCO detected 97.9% of genes as complete and single-copy, OMArk identified 96.97% of conserved Hierarchical Orthologous Groups (HOGs), and PSAURON reported a global score of 99.3 across all reading frames.

UCE epigenetic clock

We performed targeted bisulfite sequencing across 105 individuals and sequenced on average 4,472,876 reads per individual. The final methylation matrix based on UCEs contains a total of 7,637 CpG sites shared across all samples, each with base and alignment quality scores > 10 and with a minimum site coverage of five reads for each sample and an average sequencing depth of 585 reads/site. Analysis of methylation-age associations revealed the distribution of correlations with chronological age (Supplementary Fig. 3). The elastic net regression retained 39 CpG sites that collectively produced a strong correlation between predicted and chronological age from otolith readings (Pearson's $r = 0.94$) (Fig. S4). These CpG sites correspond to the final model trained on the full dataset. A complete list of the 39 CpG sites is provided in Supplementary Tables 1 and 2.

The cross-validation using the LOOCV resulted in an epigenetic clock model with a Pearson correlation coefficient (r) of 0.88 and a median absolute residual error (MedAE) of 0.834 years (Fig. 2).

In addition to comparing predicted epigenetic age to otolith-age, we examined its relationship with other biological variables, such as otolith weight. As shown in Fig. 3, a clear linear ($r = 0.82$) relationship was observed between predicted age and otolith weight,

consistent with the expected progressive calcification of otoliths over time.

Epigenome-wide association study (EWAS)

Applying an unadjusted significance threshold ($\alpha = 1.36 \times 10^{-11}$) restricted the analysis to the top 150 CpGs showing the strongest positive correlations with age (Fig. 4A). Among these CpGs sites, the main signals were detected at chr17.1_14176962 ($P = 4.6 \times 10^{-27}$) and chr17.1_14176951 ($P = 1.0 \times 10^{-26}$). Both CpGs are located within the *six6* homeobox gene (egapx_017075) on chromosome 17 and exhibit correlation coefficients higher than 0.8 (Fig. 4B). One of the top 10 CpGs is located in a member of the Six/sine oculis family of homeobox-containing transcription factors, chr14.1_22159675 ($P = 8.724690 \times 10^{-19}$) in *six3a* homeobox with a correlation coefficient exceeding 0.73 (Fig. 4C). As *six3a* and *six6* are respectively in chromosome 14 and chromosome 17 from the de novo albacore genome, their consistent age-related gain of methylation is not due to physical proximity (Fig. 4A).

The CpG site with the highest negative correlation ($r < -0.71$) (Fig. 4D) with age is located on chromosome 3, is proximal to the *lmx1bb* gene (Fig. 4A).

For the functional enrichment analysis of age-related CpG sites we sought to identify biological processes and pathways annotated by the top 150 age-related CpG sites using a GREAT-like approach.

Enrichment analysis revealed that 'Anatomical structure development' was the sole significant category, identified exclusively among the top 150 CpG sites that lost methylation with age ($P = 2.59 \times 10^{-2}$) (Fig. 5).

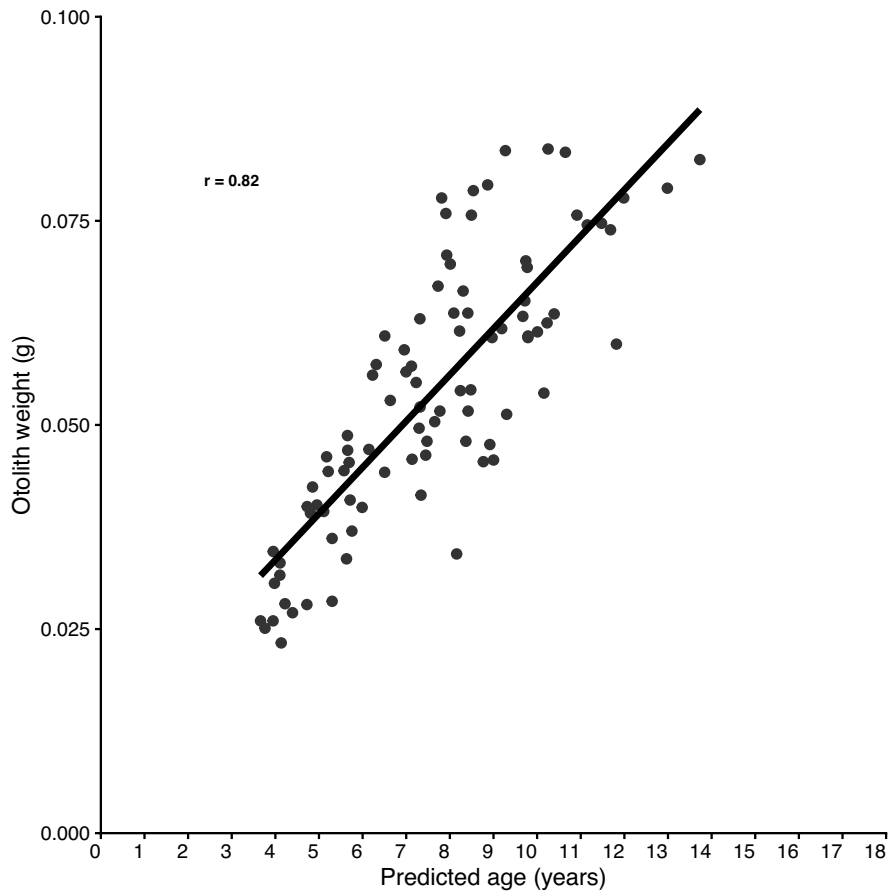

Fig. 3 Relationship between otolith weight (g) and predicted age (years) with a linear model (dashed grey line)

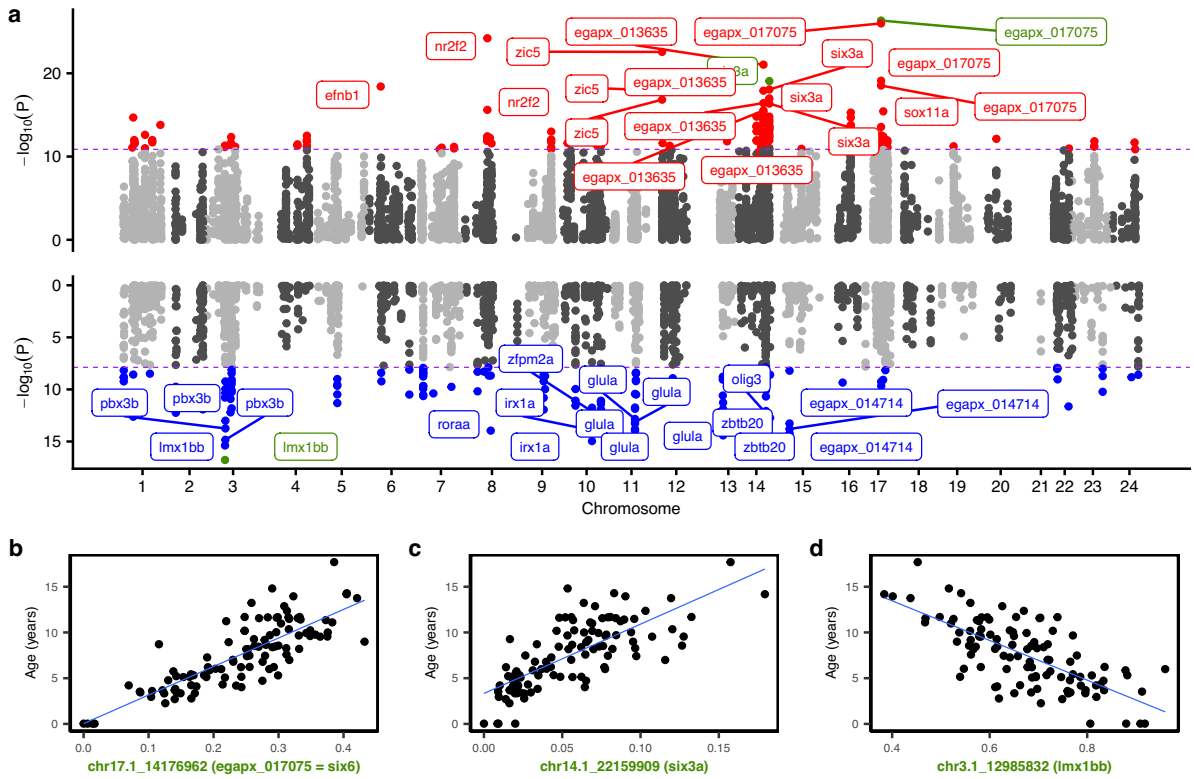

Fig. 4 **A** Meta-analysis − log10 (*P* values) for age-related CpG sites (annotated by proximal genes) on chromosomes from de novo albacore genome. Top and bottom, CpG sites that gain or lose methylation with age, respectively. CpG sites in red and blue denote highly significant positive and negative age correlation ($P_{Positive} < 1.36 \times 10^{-11}$ and $P_{Negative} < 1.32 \times 10^{-.08}$), respectively. **B**–**D** Scatterplot of **B** chr17.1_14176962, **C** chr14.1_22159909, and **D** chr3.1_12985832 versus chronological age (years)

Discussion

UCE epigenetic clock

Accurately determining the age structure and growth parameters of fish populations is essential for effective monitoring, assessment, and conservation strategies in wildlife management [1, 61–63]. In 1999, Campana and Thorrold estimated that over 800,000 otoliths were analyzed annually across the globe for age determination, covering both exploited and threatened species [6, 64]. While otolith-based aging remains widely used, it is inherently lethal, requires access to the whole fish (or at least the head), can be technically demanding, and not always feasible, particularly for high-value or protected species. By contrast, epigenetic clocks offer a promising non-lethal alternative for age estimation. With the continuous reduction in DNA sequencing costs, these molecular approaches are becoming increasingly accessible for ecological and fisheries management applications. Moreover, muscle tissue required for epigenetic analysis is easier to collect in the field, requires no specialized dissection skills, and can often be obtained from live animals. In fish, minimally invasive biopsies are particularly feasible for muscle and fin tissue, which can be sampled with limited handling time and low post-release mortality [65, 66]. Such procedures are already widely implemented in population genetic and tagging programs, indicating that the logistical framework for non-lethal tissue sampling is well established. Once established, epigenetic clocks are particularly valuable for taxa that are challenging to age reliably, especially for non-specialists. This is the case for groups such as elasmobranchs and many threatened or endangered species, where

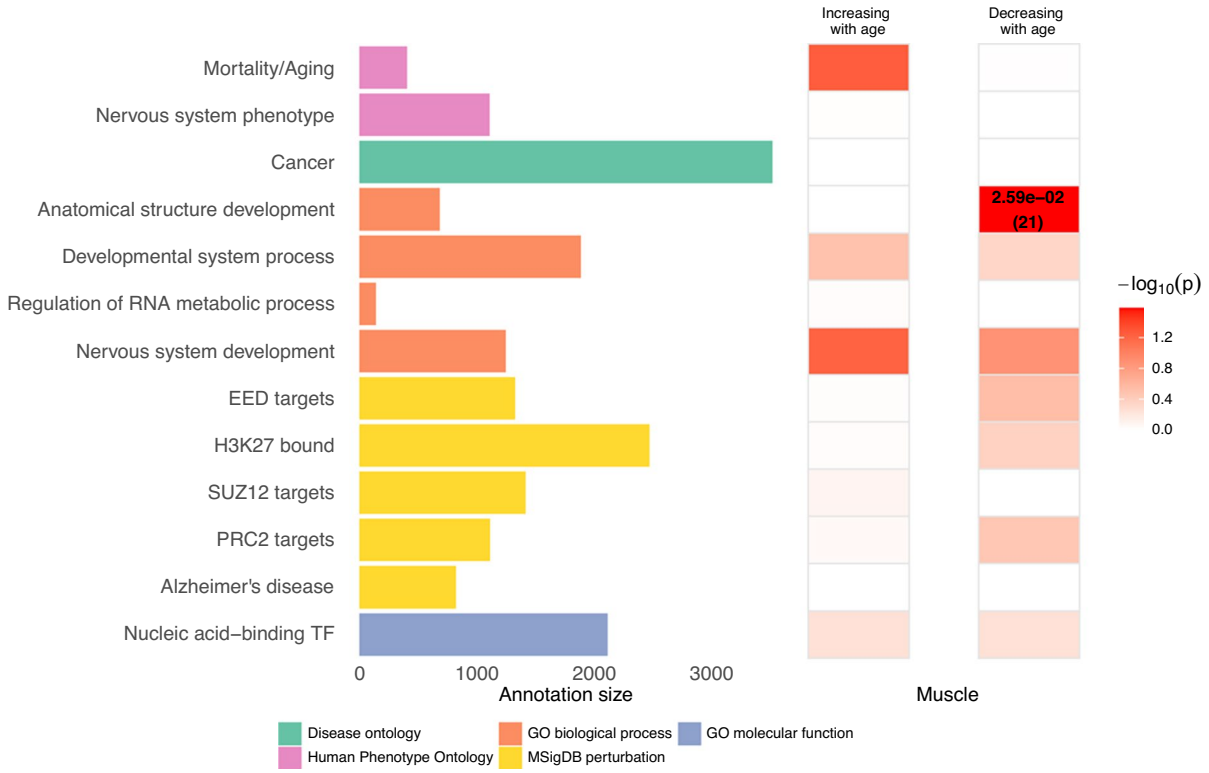

Fig. 5 Biological pathways and functional gene sets enriched in age-related CpG sites

traditional ageing methods are invasive (vertebrae or otoliths) and require specialized expertise. While building such a clock still requires access to individuals spanning the full age range, once developed, the approach circumvents these limitations and provides a practical and non-lethal tool for aging individuals in future studies. The present UCE-based clock for albacore tuna shows compelling performance with a significant correlation (Pearson's $R = 0.88$; MedAE = 0.834 years) between chronological and predicted age. This outcome is particularly promising, as it targets genomic regions that are highly conserved across multiple fish species that have diverged over millions of years [38]. Among the CpG sites significantly associated with age are sites present on genes linked to the determination of adult lifespan (*taf-4*), the development of organs (e.g. *irx5a*, *pax6b*, *LBX1*). Such evolutionary conservation makes these regions ideal candidates for developing a universal epigenetic clock for fish using multiple tissues as aging is associated with multiple cellular changes that are often tissue specific [67], analogous to pan-mammalian clocks that have been successfully established in recent years [24, 26]. Such a tool would reduce the need to build species-specific models, which are often costly and dependent on large numbers of known-age individuals.

Epigenome-wide association study (EWAS)

Among the top positively age-associated CpG sites identified in the EWAS, several lie near *six6* and *six3a*. These genes are well known for their essential roles during the earliest stages of embryonic development [68]. A previous exome-sequencing and functional study has shown that *six6* helps regulate the balance between cell proliferation and differentiation early in life, and is also implicated in optic-nerve degeneration at older ages [69] while *six3a* acts within brain development and optic nerve morphogenesis. In addition to *six3a* and *six6*, several other notable gene groups were associated with CpGs showing age-related methylation patterns, including *irx1a* (chromosome 10) and *irx5a* (chromosome 1);

SOX5 (chromosome 23), *SOX11a* (chromosome 11), and *SOX21b* (chromosome 12); and *FOXP2* (chromosome 23), *FOXP4* (chromosome 4), and *FOXB1a* (chromosome 8). Notably, several genes proximal to the top 150 age-associated CpGs code for proteins with well-established functions in developmental processes, suggesting that some epigenetic signatures of aging may echo underlying developmental regulatory networks. Consistent with this idea, several CpG sites significantly correlated with age are also associated with genes encoding key developmental regulators, including *lmx1bb, zic5*, and *en2a*, further supporting a link between age-related methylation changes and conserved developmental pathways.

This result is confirmed by our GREAT-like analysis which showed a significant enrichment for 'Anatomical structure development' for negatively age-related CpG sites. However, in contrast with enrichment patterns widely documented in axolotl and mammalian aging studies the Polycomb-regulated genomic networks was not significantly enriched for albacore [26, 40, 41]. Although several age-associated CpGs overlap H3K27me3 marks and PRC2 complex targets (including SUZ12 and EED), these annotations are inferred from conserved regulatory features characterized in mammalian rather than from direct epigenomic measurements in tuna. In the absence of teleost-specific chromatin profiling data, such overlaps should therefore be interpreted cautiously, even if they did not reach statistical significance relative to the background set. Future studies integrating chromatin immunoprecipitation sequencing (ChIP-seq) data in teleost species will be required to directly assess the involvement of Polycomb-mediated regulation in fish aging. In albacore, analyses based on UCEs instead suggest that genes showing significant associations with age whether positive or negative are more frequently linked to developmental functions.

Future directions

Among the 105 samples used in this study, 101 were derived from muscle tissue, while the remaining four, corresponding to larvae, were sampled from eye tissue. It is well established that tissue type can influence DNA methylation patterns, potentially affecting the performance and transferability of epigenetic clocks [24, 26, 32]. For this reason, it would be preferable in future work to use a single tissue type, or at least for multi-tissue approach, ensure that different tissue types are evenly distributed across the full age range of the target species [26, 32].

Otolith age readings do not uniformly cover the complete age range of the species. In particular, individuals under three years of age and those older than 14 years are underrepresented (Fig. 1) due to sampling challenges in the Indian Ocean, particularly for juveniles (< 3 years old). This limited representation may slightly reduce predictive accuracy for the oldest age classes, especially beyond 13 years. As the maximum lifespan of albacore tuna is estimated to be around 20 years, expanding the dataset to better include juvenile and older individuals would enhance an already robust clock, improving its calibration and reliability across the species' full lifespan. Increasing the sample size, particularly by targeting age classes currently underrepresented, would not only help capture the full range of age-associated methylation dynamics, but also improve the generalizability of the models. Ideally, as explained by [70], at least 70 and optimally 134 samples from a single tissue type are recommended to develop a reliable epigenetic clock for a given species, in order to minimize prediction error rates.

Overall, these findings underscore the effectiveness of UCE-targeted sequencing for the development of a robust epigenetic clock for albacore tuna. While these results provide a valuable framework for age estimation of albacore tuna, future efforts should extend this strategy to a broader range of fishes. Applying and validating such epigenetic clocks across diverse Actinopterygii, and particularly within Acanthomorphs, will be essential for assessing the feasibility of establishing a more ubiquitous epigenetic clock for age determination in teleost fishes.

Acknowledgements The authors appreciated the help of all fishers and scientific observers and technicians for the collection of the albacore samples.

Author contribution Chevrier Thomas: conceptualization, methodology, formal analysis, investigation, data curation, writing – original draft, visualization, writing-review and editing. Sylvain Bonhommeau: conceptualization, project administration, investigation, resources, methodology, writing – review and editing. Michael Thompson: methodology, formal analysis, investigation, data curation, writing—review and editing Jessica Farley: methodology, formal analysis, investigation, data curation, writing—review and editing Giorgia Del Vecchio: methodology, investigation, data curation, writing—review

and editing Anne-Elise Nieblas: writing – review and editing, supervision Dominique A. Cowart: writing – review and editing, supervision Jérémie Chanut: methodology and resources Julie Imbert Nguyen: writing – review and editing, supervision. Serge Bernard: writing – review and editing, supervision. Yann Guiguen: methodology, investigation, data curation, writing-review and editing Cedric Cabau: methodology, investigation, data curation, writing-review and editing Christophe Klopp: methodology, investigation, data curation, writing-review and editing Joseph A. Zoller: conceptualization, methodology, formal analysis, investigation, data curation, writing-review and editing Steve Horvath: conceptualization, methodology, investigation, resources, writing-review and editing Robert Brooke: writing-review and editing Ake Lu: methodology, formal analysis, investigation, writing-review and editing Matteo Pellegrini: conceptualization, methodology, investigation, resources, writing-review and editing. All authors have read and finally agreed to the published version of the manuscript.

Funding This work has been funded by the EU-FEAMP TALE project (#PFEA400020DM0980001). The GERMON project has been funded by the EU FEP fund (#13/1210964/FAV1).

Data availability The raw data that support the findings of this study are available from the corresponding author upon reasonable request and with appropriate approvals. The methylation matrix and age data used for this study are available here: https://github.com/ThomasCOOOL/Albacore_epigenetic_clock. Our Albacore de novo genome assembly generated in this study is available at: https://doi.org/10.12770/5a8376da-1664-493e-9fc7-7f6460835bf5.

Code availability Codes are available here: https://github.com/ThomasCOOOL/Albacore_epigenetic_clock.

Declarations

The Regents of the University of California are the sole owner of patents and patent applications directed at epigenetic biomarkers and the mammalian methylation array platform for which Steve Horvath is a named inventor; SH is a founder and paid consultant of the non-profit Epigenetic Clock Development Foundation that licenses these patents. SH is a Principal Investigator at the Altos Labs, Cambridge Institute of Science. The other authors have non-financial and no conflicts of interest to declare.

References

1. Ono K, Licandeo R, Muradian ML, Cunningham CJ, Anderson SC, Hurtado-Ferro F, et al. The importance of length and age composition data in statistical age-structured models for marine species. ICES J Mar Sci. 2015;72:31–43. https://doi.org/10.1093/icesjms/fsu007.
2. Schaffer WM. Selection for optimal life histories: the effects of age structure. Ecology. 1974;55:291–303. https://doi.org/10.2307/1935217.
3. Western D. Size, life history and ecology in mammals. Afr J Ecol. 1979;17:185–204. https://doi.org/10.1111/j.1365-2028.1979.tb00256.x.
4. Frisk MG, Miller TJ, Fogarty MJ. Estimation and analysis of biological parameters in elasmobranch fishes: a comparative life history study. Can J Fish Aquat Sci. 2001;58:969–81. https://doi.org/10.1139/f01-051.
5. Cailliet GM, Andrews AH, Burton EJ, Watters DL, Kline DE, Ferry-Graham LA. Age determination and validation studies of marine fishes: do deep-dwellers live longer? Exp Gerontol. 2001. https://doi.org/10.1016/S0531-5565(00)00239-4.
6. Campana SE. Accuracy, precision and quality control in age determination, including a review of the use and abuse of age validation methods. J Fish Biol. 2001;59:197–242. https://doi.org/10.1111/j.1095-8649.2001.tb00127.x.
7. Goren AD, Brodie PF, Spotte S, Ray GC, Kaufman HW, Gwinnett AJ, et al. Growth layer groups (GLGs) in the teeth of an adult belukha whale (*Delphinapterus leucas*) of known age: evidence for two annual layers. Mar Mamm Sci. 1987;3:14–21. https://doi.org/10.1111/j.1748-7692.1987.tb00148.x.
8. Pannella G. Fish otoliths: daily growth layers and periodical patterns. Science. 1971. https://doi.org/10.1126/science.173.4002.1124.
9. Secor DH, Henderson-Arzapalo A, Piccoli PM. Can otolith microchemistry chart patterns of migration and habitat utilization in anadromous fishes? J Exp Mar Biol Ecol. 1995;192:15–33. https://doi.org/10.1016/0022-0981(95)00054-U.
10. Helser TE, Benson I, Erickson J, Healy J, Kastelle C, Short JA. A transformative approach to ageing fish otoliths using Fourier transform near infrared spectroscopy: a case study of eastern Bering Sea walleye pollock (*Gadus chalcogrammus*). Can J Fish Aquat Sci. 2019;76:780–9. https://doi.org/10.1139/cjfas-2018-0112.
11. Anastasiadi D, Piferrer F. A clockwork fish: age prediction using DNA methylation-based biomarkers in the European seabass. Mol Ecol. 2019. https://doi.org/10.1111/1755-0998.13111.
12. Quinn TF, Deriso RB. Quantitative fish dynamics. 1999.
13. Brunel T, Piet GJ. Is age structure a relevant criterion for the health of fish stocks? ICES J Mar Sci. 2013;70:270–83. https://doi.org/10.1093/icesjms/fss184.

14. Vitale F, Worsøe Clausen L, Ní Chonchúir G. Handbook of fish age estimation protocols and validation methods. ICES; 2019; https://doi.org/10.17895/ICES.PUB.5221
15. Boyd-Kirkup JD, Green CD, Wu G, Wang D, Han J-D. Epigenomics and the regulation of aging. Epigenomics. 2013;5:205–27. https://doi.org/10.2217/epi.13.5.
16. Booth LN, Brunet A. The aging epigenome. Mol Cell. 2016;62:728–44. https://doi.org/10.1016/j.molcel.2016.05.013.
17. Simide R, Angelier F, Gaillard S, Stier A. Age and heat stress as determinants of telomere length in a long-lived fish, the Siberian sturgeon. Physiol Biochem Zool. 2016;89:441–7. https://doi.org/10.1086/687378.
18. Sauer DJ, Heidinger BJ, Kittilson JD, Lackmann AR, Clark ME. No evidence of physiological declines with age in an extremely long-lived fish. Sci Rep. 2021;11:9065. https://doi.org/10.1038/s41598-021-88626-5.
19. Bell CG, Lowe R, Adams PD, Baccarelli AA, Beck S, Bell JT, et al. DNA methylation aging clocks: challenges and recommendations. Genome Biol. 2019;20:249. https://doi.org/10.1186/s13059-019-1824-y.
20. Chen L, Ganz PA, Sehl ME. DNA methylation, aging, and cancer risk: a mini-review. Front Bioinforma. 2022;2:847629. https://doi.org/10.3389/fbinf.2022.847629.
21. Horvath S, Raj K. DNA methylation-based biomarkers and the epigenetic clock theory of ageing. Nat Rev Genet. 2018;19:371–84. https://doi.org/10.1038/s41576-018-0004-3.
22. Unnikrishnan A, Freeman WM, Jackson J, Wren JD, Porter H, Richardson A. The role of DNA methylation in epigenetics of aging. Pharmacol Ther. 2019;195:172–85. https://doi.org/10.1016/j.pharmthera.2018.11.001.
23. Wang K, Liu H, Hu Q, Wang L, Liu J, Zheng Z, et al. Epigenetic regulation of aging: implications for interventions of aging and diseases. Signal Transduct Target Ther. 2022;7:374. https://doi.org/10.1038/s41392-022-01211-8.
24. Arneson A, Haghani A, Thompson MJ, Pellegrini M, Kwon SB, Vu H, et al. A mammalian methylation array for profiling methylation levels at conserved sequences. Nat Commun. 2022;13:783. https://doi.org/10.1038/s41467-022-28355-z.
25. Horvath S. DNA methylation age of human tissues and cell types. Genome Biol. 2013;14:3156. https://doi.org/10.1186/gb-2013-14-10-r115.
26. Lu AT, Fei Z, Haghani A, Robeck TR, Zoller JA, Li CZ, et al. Universal DNA methylation age across mammalian tissues. Nature Aging. 2023;3:1144–66. https://doi.org/10.1038/s43587-023-00462-6.
27. Teschendorff AE, Horvath S. Epigenetic ageing clocks: statistical methods and emerging computational challenges. Nat Rev Genet. 2025;26:350–68. https://doi.org/10.1038/s41576-024-00807-w.
28. Polanowski AM, Robbins J, Chandler D, Jarman SN. Epigenetic estimation of age in humpback whales. Mol Ecol Resour. 2014;14:976–87. https://doi.org/10.1111/1755-0998.12247.
29. Bors EK, Baker CS, Wade PR, O'Neill KB, Shelden KEW, Thompson MJ, et al. An epigenetic clock to estimate the age of living beluga whales. Evol Appl. 2021;14:1263–73. https://doi.org/10.1111/eva.13195.
30. Mayne B, Korbie D, Kenchington L, Ezzy B, Berry O, Jarman S. A DNA methylation age predictor for zebrafish. Aging. 2020;12:24817–35. https://doi.org/10.18632/aging.202400.
31. Weber DN, Fields AT, Patterson WF, Barnett BK, Hollenbeck CM, Portnoy DS. Novel epigenetic age estimation in wild-caught Gulf of Mexico reef fishes. Can J Fish Aquat Sci. 2022;79:1–5. https://doi.org/10.1139/cjfas-2021-0240.
32. Weber DN, Fields AT, Chamberlin DW, Patterson WF, Portnoy DS. Epigenetic age estimation in a long-lived, deepwater scorpionfish: insights into epigenetic clock development. Can J Fish Aquat Sci. 2024;81:620–31. https://doi.org/10.1139/cjfas-2023-0296.
33. Weber DN, Wyffels JT, Buckner C, George R, Latson FE, LePage V, et al. Noninvasive, epigenetic age estimation in an elasmobranch, the cownose ray (*Rhinoptera bonasus*). Sci Rep. 2024;14:26261. https://doi.org/10.1038/s41598-024-78004-2.
34. Farley J, Eveson JP, Krusic-Golub K, Clear NP, Sanchez C, Nicol SJ. Jesstimation: a novel approach for estimating more accurate fish ages from otolith zone counts and measurements. Fish Res. 2025;288:107463. https://doi.org/10.1016/j.fishres.2025.107463.
35. Farley J, Eveson P, Bonhommeau S, Dhurmeea Z, West W, Bodin N. Growth of albacore tuna (Thunnus alalunga) in the western Indian Ocean using direct age estimates. 2019. IOTC-2019-WPTmT07(DP)-21_Rev1
36. Maleszka R. Is the concept of mammalian epigenetic clocks universal and applicable to invertebrates? Front Genet. 2025;16:1633921. https://doi.org/10.3389/fgene.2025.1633921.
37. Alfaro ME, Faircloth BC, Harrington RC, Sorenson L, Friedman M, Thacker CE, et al. Explosive diversification of marine fishes at the Cretaceous–Palaeogene boundary. Nat Ecol Evol. 2018;2:688–96. https://doi.org/10.1038/s41559-018-0494-6.
38. Faircloth BC, Sorenson L, Santini F, Alfaro ME. A phylogenomic perspective on the radiation of ray-finned fishes based upon targeted sequencing of ultraconserved elements (UCEs). PLoS One. 2013;8:e65923. https://doi.org/10.1371/journal.pone.0065923.
39. Nakamura Y, Higuchi K, Kumon K, Yasuike M, Takahashi T, Gen K, et al. Prediction of the sex-associated genomic region in tunas (Thunnus Fishes). Int J Genomics. 2021;2021:14. https://doi.org/10.1155/2021/7226353.
40. Haluza Y, Zoller JA, Lu AT, Walters HE, Lachnit M, Lowe R, et al. Axolotl epigenetic clocks offer insights into the nature of negligible senescence. BioRxiv. 2024;10:2024–09. https://doi.org/10.1101/2024.09.09.611397.
41. Parson K, Haghani A, Zoller J, Lu A, Fei Z, Ferguson S, et al. DNA methylation-based biomarkers for ageing long-lived cetaceans. Mol Ecol. 2023. https://doi.org/10.1111/1755-0998.13791.
42. Nikolic N, Puech A, Chouvelon T, Munschy C, Bodin N, Brach-Papa C, Potier M, West W, Knoery J, Zudaire I, Dhurmeea Z. Projet GERMON. Structure génétique et migration du thon Germon. https://doi.org/10.13155/40461
43. Lee G-Y, Suh S-M, Lee Y-M, Kim H-Y. Multiplex PCR assay for simultaneous identification of five types of tuna (*Katsuwonus pelamis, Thunnus alalunga, T. albacares, T.*

obesus and T. thynnus). Foods. 2022;11:280. https://doi.org/10.3390/foods11030280.
44. Cheng H, Concepcion GT, Feng X, Zhang H, Li H. Haplotype-resolved de novo assembly using phased assembly graphs with hifiasm. Nat Methods. 2021;18:170–5. https://doi.org/10.1038/s41592-020-01056-5.
45. Guan D, McCarthy SA, Wood J, Howe K, Wang Y, Durbin R. Identifying and removing haplotypic duplication in primary genome assemblies. Bioinformatics. 2020;36:2896. https://doi.org/10.1093/bioinformatics/btaa025.
46. Durand NC, Shamim MS, Machol I, Rao SSP, Huntley MH, Lander ES, et al. Juicer provides a one-click system for analyzing loop-resolution Hi-C experiments. Cell Syst. 2016;3:95. https://doi.org/10.1016/j.cels.2016.07.002.
47. Dudchenko O, Batra SS, Omer AD, Nyquist SK, Hoeger M, Durand NC, et al. De novo assembly of the *Aedes aegypti* genome using Hi-C yields chromosome-length scaffolds. Science. 2017;356:92. https://doi.org/10.1126/science.aal3327.
48. Durand NC, Robinson JT, Shamim MS, Machol I, Mesirov JP, Lander ES, et al. Juicebox provides a visualization system for Hi-C contact maps with unlimited zoom. Cell Syst. 2016;3:99–101. https://doi.org/10.1016/j.cels.2015.07.012.
49. Astashyn A, Tvedte ES, Sweeney D, Sapojnikov V, Bouk N, Joukov V, et al. Rapid and sensitive detection of genome contamination at scale with FCS-GX. Genome Biol. 2024;25:60. https://doi.org/10.1186/s13059-024-03198-7.
50. Manni M, Berkeley MR, Seppey M, Simão FA, Zdobnov EM. BUSCO update: novel and streamlined workflows along with broader and deeper phylogenetic coverage for scoring of eukaryotic, prokaryotic, and viral genomes. Mol Biol Evol. 2021;38:4647. https://doi.org/10.1093/molbev/msab199.
51. Nevers Y, Warwick Vesztrocy A, Rossier V, Train C-M, Altenhoff A, Dessimoz C, et al. Quality assessment of gene repertoire annotations with OMArk. Nat Biotechnol. 2025;43:124. https://doi.org/10.1038/s41587-024-02147-w.
52. Sommer MJ, Zimin AV, Salzberg SL. Psauron: a tool for assessing protein annotation across a broad range of species. NAR Genom Bioinform. 2025;7:lqae189. https://doi.org/10.1093/nargab/lqae189.
53. Farrell C, Thompson M, Tosevska A, Oyetunde A, Pellegrini M. Bisulfite bolt: a bisulfite sequencing analysis platform. Gigascience. 2021;10:giab033. https://doi.org/10.1093/gigascience/giab033.
54. Chen S. Ultrafast one-pass FASTQ data preprocessing, quality control, and deduplication using fastp. iMeta. 2023. https://doi.org/10.1002/imt2.107.
55. Li H, Durbin R. Fast and accurate long-read alignment with Burrows–Wheeler transform. Bioinformatics. 2010;26:589–95. https://doi.org/10.1093/bioinformatics/btp698.
56. Li H. Aligning sequence reads, clone sequences and assembly contigs with BWA-MEM. arXiv. 2013. https://doi.org/10.48550/arXiv.1303.3997.
57. Danecek P, Bonfield JK, Liddle J, Marshall J, Ohan V, Pollard MO, et al. Twelve years of SAMtools and BCFtools. Gigascience. 2021;10:giab008. https://doi.org/10.1093/gigascience/giab008.
58. Zoller J, Horvath S. MammalMethylClock R package: software for DNA methylation-based epigenetic clocks in mammals. Bioinformatics. 2024;40:btae280. https://doi.org/10.1093/bioinformatics/btae280.
59. Langfelder P, Horvath S. WGCNA: an R package for weighted correlation network analysis. BMC Bioinformatics. 2008;9:559. https://doi.org/10.1186/1471-2105-9-559.
60. Lee Y-H, Yen T-B, Chen C-F, Tseng M-C. Variation in the karyotype, cytochrome b gene, and 5S rDNA of four *thunnus* (Perciformes, Scombridae) tunas. Zool Stud. 2018. https://doi.org/10.6620/ZS.2018.57-34.
61. Hoenig JM. Empirical use of longevity data to estimate mortality rates. 1983;Fishery Bulletin:898-903.
62. Bravington MV, Grewe PM, Davies CR. Absolute abundance of southern bluefin tuna estimated by close-kin mark-recapture. Nat Commun. 2016;7:13162. https://doi.org/10.1038/ncomms13162.
63. Tabak MA, Webb CT, Miller RS. Propagule size and structure, life history, and environmental conditions affect establishment success of an invasive species. Sci Rep. 2018;8:10313. https://doi.org/10.1038/s41598-018-28654-w.
64. Thorrold SR, Hare JA. Otolith applications in reef fish ecology. In: Coral Reef Fishes. Elsevier; 2002. p. 243–64. https://doi.org/10.1016/B978-012615185-5/50015-3.
65. Vejřík L, Vejříková I, Sajdlová Z, Kočvara L, Kolařík T, Bartoň D, et al. A non-lethal stable isotope analysis of valued freshwater predatory fish using blood and fin tissues as alternatives to muscle tissue. PLoS ONE. 2024;19:e0297070. https://doi.org/10.1371/journal.pone.0297070.
66. Henderson CJ, Stevens TF, Lee SY. Assessing the suitability of a non-lethal biopsy punch for sampling fish muscle tissue. Fish Physiol Biochem. 2016;42:1521–6. https://doi.org/10.1007/s10695-016-0237-z.
67. Ferrucci L, Gonzalez-Freire M, Fabbri E, Simonsick E, Tanaka T, Moore Z, et al. Measuring biological aging in humans: a quest. Aging Cell. 2020;19:e13080. https://doi.org/10.1111/acel.13080.
68. Conte I, Morcillo J, Bovolenta P. <article-title update="added"> Comparative analysis of *Six3* and *Six6* distribution in the developing and adult mouse brain. Dev Dyn. 2005;234(3):718–25. https://doi.org/10.1002/dvdy.20463.
69. Iglesias AI, Springelkamp H, Van Der Linde H, Severijnen L-A, Amin N, Oostra B, et al. Exome sequencing and functional analyses suggest that SIX6 is a gene involved in an altered proliferation–differentiation balance early in life and optic nerve degeneration at old age. Hum Mol Genet. 2014;23:1320–32. https://doi.org/10.1093/hmg/ddt522.
70. Mayne B, Berry O, Jarman S. Optimal sample size for calibrating DNA methylation age estimators. Mol Ecol Resour. 2021;21:2316–23. https://doi.org/10.1111/1755-0998.13437.